文章编号：1001-9014(2019)06-0716-06

DOI:10.11972/j.issn.1001-9014.2019.06.006

An angle-independent broadband terahertz bandstop filter based on compact cross-shaped array

NING Yu-Peng, LOU Shu-Qin*, JIA Hong-Zhi, LIU Xi-Dan, SUN Pu

(School of Electronic and Information Engineering, Beijing Jiaotong University, Beijing 100044, China)

Abstract: In this paper, a design of compact array which can excite anti-symmetric mode on special frequency selective surfaces is introduced. Based on compact cross-shaped array, we proposed an angle independent broadband terahertz (THz) bandstop filter with compact cross-shaped array. The compact cross-shaped array is composed of two layers of cross-shaped metal array, in which the center of every cross-shaped unit cell in second layer is arranged at the center of four cross-shaped unit cells in the first layer. Numerical results demonstrate that the compact array can efficiently increase the received area of the filter and excite an additional resonant mode. Compared with traditional repetitive structure, the proposed filter based on compact array has great promotion in bandwidth, sharpness and stopband depth. The filter has a notable filter capability with 10 dB bandwidth of 0.75 THz at the central frequency of 1.2 THz and incident angle insensitive range from 0° to 60°. Furthermore, the proposed compact array is flexible and can be extended for different unit cells, such as Jerusalem cross, I-shaped, Ⅱ-shaped structures, etc.

Key words: terahertz filter, frequency selective surface, compact array, angle independent, anti-symmetric mode

PACS: 78.68.+m, 42.15.Eq, 85.50.-n

基于紧凑十字阵列的角度无关的宽带太赫兹带阻滤波器

宁玉鹏, 娄淑琴*, 贾洪志, 刘锡丹, 孙 璞

(北京交通大学 电子信息工程学院,北京 100044)

摘要:介绍了一种可以在一些特殊的频率选择表面上激发额外的反对称模式的紧凑阵列设计.基于这种设计,本文提出了一种角度无关的宽带太赫兹(THz)带阻滤波器.紧凑十字架阵列由两层十字架金属阵列组成,其中第二层金属十字架的中心与第一层四个金属十字架单元的中心对齐.数值结果显示紧凑阵列可以激发出一种额外的谐振模式.与传统的周期设计相比,基于紧凑阵列的滤波器在带宽、通带平坦度和阻带衰减均有很大的性能提升.提出的滤波器具有良好的滤波能力,其在1.2 THz的中心频率处具有0.75 THz的10 dB带宽且在0°~60°的范围内对角度不敏感.此外,紧凑阵列可以被拓展运用到多种不同的结构,如耶路撒冷十字架结构,I型以及II型等结构.

关 键 词:太赫兹滤波器;频率选择表面;紧凑阵列;角度无关;反对称模式

中图分类号:TN214 **文献标识码**:A

Introduction

Owing to terahertz (THz) wave's unique electromagnetic features, THz frequency range has attracted enormous interest in the past decades which lead to extensive studies in various areas, such as high-speed communication[1-2], security[3], biomedical imaging[4-6] and nondestructive testing[7]. THz wave filters are indispensable functional device in terahertz sensing, communication, and imaging system[8]. Due to most of natural materials almost having no electromagnetic (EM) response for THz waves, it is a challenge for developing THz filter with high performance. With the coming of metamaterials (MMs), which have strong EM response to THz

Received date: 2019-05-20, **revised date**: 2019-07-14 **收稿日期**:2019-05-20,**修回日期**:2019-07-14

Foundation items: Supported by National Natural Science Foundation of China (NSFC) (61575016).

Biography: NING Yu-Peng(1996-), male, Shaodong China, master. Research area involves terahertz theory and devices. E-mail: 17120098@bjtu.edu.cn

* **Corresponding author**: E-mail: shqlou@bjtu.edu.cn

waves[9-10], it offers the possibility for designing novel THz filter. The frequency selective surfaces (FSSs) based on MMs possess considerable potential in THz filter design. Through exciting resonance between the free electrons in the metal and the optical photons from the incident EM waves, an extraordinary transmission spectrum can be realized by FSS[11]. The filter based on FSS is constructed from metallic particles or grids which exhibit certain filter characteristics and its optical characteristics are determined by its dimensions[11], geometric structure[14-15], metal thickness[16] and materials[17]. By means of appropriate optimizing these parameters of designed filter, the transmission spectrum of THz filter can be tailored[12-13].

The FSS with the structure of cross-shaped metal array reveals good performance in polarization-insensitivity due to its rotational symmetry. However, compared with MMs like split-ring resonators (SRRs) or other ring-like resonators, cross-shaped FSS cannot excite multiple resonance when it is used to construct multi-layer THz filter. Additionally, the bandwidth of filter based on FSS is limited because of its strong EM resonance. Hence, in order to overcome these problems, various designs have been proposed like complementary cross-shaped resonator [14] and composite metamaterial [18-19]. Besides, in the previous studies, the design of different metal array distributed in different layer were often adopted to obtain wider bandwidth. For instance, in 2011, by using improved structure of cross-shaped structure, Chiang *et al*. presented a THz band-pass filter which can excite multiple resonances to acquire 500 GHz bandwidth passband (the full width at half maximum of the transmitted power) [18]. However, its transmission coefficient in all band is less than 0.7. In 2015, by using two layers of different metallic arrays, a second-order cross-shaped THz filter based on FSS was formed [14]. It possessed a 200 GHz bandwidth with outstanding gain. In 2017, Meng Gao *et al*. reported a hybrid miniaturized-element FSS by scraping three layers of different metallic arrays to obtain better filtering performance [26]. But the current methods to obtain multiple resonances and wider bandwidth need the more complicated structure. In this paper, by simply adjusting the position of second metallic layer, we proposed a novel filter that can excite multiple resonances. The 10 dB bandwidth can be extended to 750 GHz. At the meantime, in contrast to the previous filters, the structure of proposed filter is also greatly simplified.

In another way, owing to the complexity of real application environment, THz filter is also required to maintain its transmission spectrum for a complex incidence condition. In recent years, several angle-insensitive THz filters have been proposed[20-23]. Generally, thanks to the rotational symmetry, concentric ring resonators and cross-shaped FSSs have innate advantage in realizing polarization-independent and wide-angle THz filter. For example, in 2011, on the basis of two concentric ring resonators with interdigitated fingers placed between the rings, Ibraheem Al-Naib et al. demonstrated a polarization and angle independent THz MM with high quality-factors [20]. However, the application of designed MM is limited due to its performance in the bandwidth and insertion loss. Besides, by using triple-ring structure, Limei Qi et al. obtained a multiband THz filter with polarization-independence and insensitivity to incidence angles[22]. But the proposed filter is restricted by bandpass flatness. In 2017, by patterning cross-shaped Zeonor FSS on thin low-loss polymer substrates, A. Ferraro et al. reported similar results [21]. But it also appears narrow bandwidth and low gain. Therefore, the performance of THz filters with polarization-independence and insensitivity to incident angles need further improved.

In this paper, by using compact array, we proposed a broadband cross-shaped THz filter with second-order response and insensitivity to incident angle. The filter is composed of two layers of staggered metallic array. And compared with traditional repetitive structure, the second layer complements the vacant space of first layer when viewed from the top view, which means that the second layer has more possibility to receive perpendicular incident THz waves. Furthermore, this design can excite two resonant modes while the same structure with traditional repetitive design can only excite one resonant mode. Based on this design, the 10 dB bandwidth of designed filter can also be greatly expanded from 510 GHz to 750 GHz and its stopband depth is also deepened about 20 dB. Besides, by analyzing the surface currents density of the filter, we manifested the mechanism of how the compact array enhance the filtering performance of designed filter. Numerical results demonstrate that the designed filter with compact array can efficiently multiply the receiving area of incident THz wave and an extra resonant mode can be excited by introducing structural asymmetry. Besides, the proposed THz filter is insensitive to angle and also independent on polarization owing to rotational symmetry of cross-shaped resonator. In addition, the numerical results also indicate that this compact array scheme can be used in other structure to improve the performance of the filter, such as bandwidth, stopband depth, and rising and trailing edges.

1 Structure of designed filter

The designed THz filter is basically based on cross-shaped resonator with compact array, as shown in Fig. 1 (a). Looking down from top to the bottom, the second layer of designed filter make up the vacant space of the first layer. Compared with traditional repetitive structure[14,18-19], two-layer metal arrays based on compact structure will be much more efficient when receiving THz waves. Figure 1(b) shows the unit cell of designed THz filter based on compact structure. All of the metal parts are embedded in a polyimide substrate. The metallic layer is a 0.6 μm thick Au film whose frequency independent conductivity is s=4.09×10^7 S/m. The width w of cross-shaped resonators is set as 16 μm. From top to the bottom, the thickness of the polyimide substrate are h_1 = 10 μm, h_2 = 26 μm, h_3 = 10 μm, respectively. The period of this structure is $P_x = P_y$ = 76 μm while the length of the crossarm is K = 72 μm. From the previous report[25],

the peak wavelength of transmission spectrum is determined by the length of the crossarm. In addition, strong coupling can be obtained when the cross-shaped metal parts are close to each other. Thus, the period of designed filter was set very close to the length of crossarm, which leads to a better performance in its bandwidth. Figure 1(c) shows the unit cell of a traditional repetitive band-stop THz filter with same parameters.

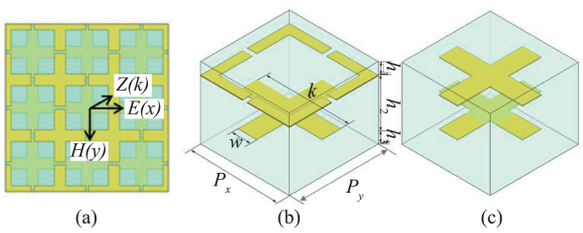

Fig. 1 Structure of the proposed filter (a) Top view of designed filter based on compact array, (b) the unit cell of the designed filter based on compact array, and (c) the unit cell of a traditional band-stop THz filter with same parameters
图1 滤波器的结构 (a)基于紧凑阵列的滤波器的俯视图,(b)基于紧凑阵列的滤波器的单元结构,(c)具有相同结构参数的传统设计滤波器的单元结构

2 Results and discussions

Finite-difference time-domain method was used to simulate the properties of the design filters; periodic boundary conditions were set in the x and y directions, and open space boundary conditions were used in the z-direction. The EM waves with the electric field parallel to the x-axis was perpendicularly incident on the designed filter.

Figure 2 shows the transmission spectrum of designed filter based on compact array and traditional repetitive array. It can be seen from Fig. 2 that the filter with compact array excites two resonant points at f_m = 0.97 THz, and f_e = 1.39 THz while the traditional design only excites one resonance point at f_l = 1.075 THz. The 10 dB bandwidth of filter is 750 GHz, which is 220 GHz wider than that of traditional structure. Moreover, the filter with compact array has better performance in slope of rising and trailing edges than the traditional one; the slope of rising edge increases from 77 dB/THz to 258 dB/THz and that of trailing edge arises from 61 dB/THz to 180 dB/THz. Besides, the stopband depth (max value) of the proposed filter is further deepened from 28 dB of traditional structure to 48 dB.

In order to clearly interpret the physics mechanism of high performance, the surface current density of the proposed filter and traditional structure at their resonant points is shown in Fig. 3. It can be found from Fig. 3 that the second metal layer of the proposed filter has stronger current than that of traditional design while the surface current on the first layer of these two filters are basically at same level (not shown here). This also means that a much stronger resonance occurs on the second layer of designed filter with compact array. According to the previous report[27], THz filter based on FSS will induce surface current when receiving THz waves and it will transform the energy of EM waves into the ohmic loss of electrons, thus the THz waves can be filtered out. The more energy to be transformed into the ohmic loss of electrons, the stronger surface currents will be. On this basis, the phenomenon can be explained that the filter with compact array has better performance in stopband depth.

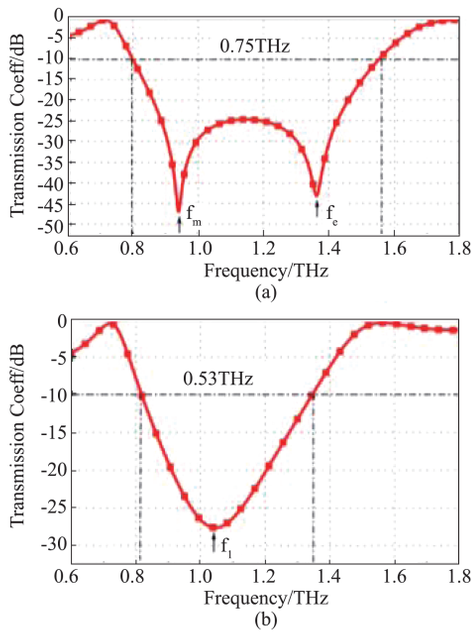

Fig. 2 Transmission coefficient of two designed filters (a) transmission spectrum of filter with compact array, and (b) transmission spectrum of filter with traditional repetitive design
图2 两种滤波器的透射系数 (a)基于紧凑阵列的滤波器的透射谱,(b)基于传统重复结构的滤波器的透射谱

In traditional repetitive structure, the second layer was always covered by the first one in the space. In most instances, the second layer of designed filter can only receive a small part of THz waves. Through using compact array, the metal arrays distributed more compactly, and every metal layer has more possibility to receive THz waves. This can be proved by the simulation result in Fig. 3. Owing to a better capacity of receiving EM waves, the coupling resonance is distinctly enhanced, causing a deeper attenuation. Meanwhile, the enhanced resonance significantly increases the loss of the microstructures at its resonant frequencies, manifesting itself as greater effective electrical resistance within the stopband. From the equivalent electric circuit model for MM[31-32], the bandwidth of the metamaterial-based filter can be determined as R_{eff}/L, where R_{eff} is the effective electrical resistance and L represents the inductance. Hence, the enhanced resonance means that R_{eff} is increased and thus a broader stopband can be obtained.

Moreover, as shown in Fig. 2, the proposed filter has two resonant points at f_m and f_e while the filter with traditional design only excites one resonant mode. With the excitation of an additional resonant point, its bandwidth and the edges are optimized. To figure out how this new resonant mode appears, we simulate its respective

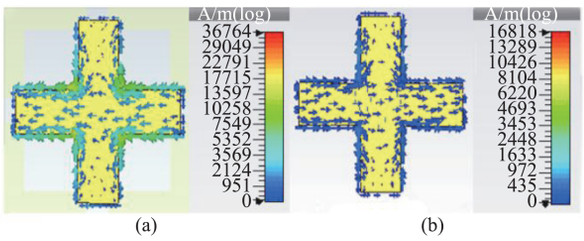

Fig. 3 Surface current density on second metal layer of designed filter (a) currents of compact filter at f_m, and (b) currents of traditional filter at f_1
图3 滤波器第二层金属的表面电流密度(a)紧凑设计滤波器在f_m处的表面电流,(b)传统设计滤波器在f_1处的表面电流

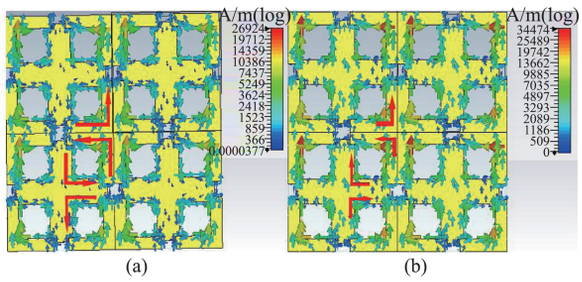

Fig. 4 The resonant modes of designed filter based on compact array (a) resonant mode at f_m, and (b) resonant mode at f_e
图4 基于紧凑阵列的滤波器的谐振模式(a)在f_m处的谐振模式,(b)在f_e处谐振模式

resonant modes and coupled behaviors at two resonant frequencies. As can be found from Fig. 4, at first resonant frequency f_m, the induced currents of upper and bottom metallic layers propagate along the opposite direction since they are excited by symmetric mode, which is also the same as the mode excited in traditional design at f_1 in Fig. 2. While at second resonant frequency f_e, the induced currents of upper and bottom metallic layers propagate along the identical direction and mainly distributed at the edges of the crossarm. This mode belongs to a kind of anti-symmetric mode. In previous studies, several filters with a broken structural symmetry, allowing weak coupling to free space, can excite a novel mode and this mode is called as anti-symmetric mode [28-30]. Additionally, as an EM mode that is weakly coupled to free space, it allows to induce high-quality resonances in very thin structure. In this paper, the compact array can be considered introducing structural asymmetry along the incident direction. This structural asymmetry can excite an extra high-quality resonant mode at f_e. The resonance behavior of currents is also consistent with that reported in Ref. 29. The additional mode at f_e and anti-symmetric mode seem to be homologous from source to behaviors.

As shown in Fig. 4, the resonant modes excited by their induced currents at f_m and f_e coincide with anti-symmetric and symmetric modes. Compared with traditional design, the proposed filter with compact array can excite an additional resonant mode which caused a better performance in bandwidth and the slope of cutting edges. Normally, a multi-layer filter based on SRR or ring structure can excite multiple resonant modes because of the coupling between different layers of metallic arrays. Based on this strategy, the performance of filter can be optimized by increasing the number of layers in many cases[33-34]. However, this characteristic does not appear on the filter based on cross-sharped FSS. Hence, in many cases, complicated structure like complementary cross-shaped resonator and composite metamaterial are widely used in THz filter to achieve multiple resonant modes[14,18-19,26]. Here, we use a simple method of compact array achieving multiple resonances.

Due to the rotational symmetry, the designed filter is polarization independent. Another marvelous behavior can be illustrated in Fig. 5, in which the transmission coefficient as a function of the frequency and the incidence angle is shown. It can be observed from Fig. 5 that the resonant frequency and the bandwidth have slight change for the incident angle varied from 0°to 60°. For every 15° increment in the incident angle, the first resonant point f_m shifts towards the low frequency by the amount movement of 3 GHz, 14 GHz, 16 GHz, and 17 GHz, respectively; and the second one f_e shifts towards the high frequency by the amount movement of 3 GHz, 13 GHz, 12 GHz, and 17 GHz, respectively. As a result, the 10 dB bandwidth can be widened from 0.750 THz to to 0.798 THz. Meanwhile, their sidelobe suppression are nearly constant in the angle range of 0° to 60°. This excellent performance mainly attributes to its proper structural design. Generally, the multilayer THz filters based on ring-like resonator require the accurate alignment between layers since their transmission spectrum mainly depends on the coupling behavior of different metal layers. If the incident angle changes, there is an equivalent change for the alignment of layers, causing the performance of the filter degradation. However, the multilayer cross-shaped filter mainly depends on the resonant behavior of individual metal layer rather than coupling between layers. Moreover, as a result of staggered arrangement of metal patches, the second layer of designed filter occupied the vacant space of the first metal layer, causing better reception of EM waves. Thus, the filter is not particularly sensitive to incident angle. In addition, the transmission spectrum of the filter under different incident conditions is also affected by its structural parameters of metal resonator and substrate. Among them, the most influential factor are length, width of cross arm and vertical distance between two-layer metal resonators. Therefore, by choosing suitable parameters, the best performance of the filter insensitive to the incident angle can be achieved.

The scheme of compact array is also suitable to construct new high-performance filter with other commonly used resonator as a unit cell. Figure 6 shows several commonly used resonator cells, including Jerusalem cross resonator, I-shaped and II-shaped resonator. They are arranged as compact array and traditional repetitive structure with double metal layers and the same substrate structure parameters in Fig. 1 except different shape and size of metal unit cell. In order to clearly compare the performance of these filters, we summarize the main performance parameters of these filters in Table 1, in which

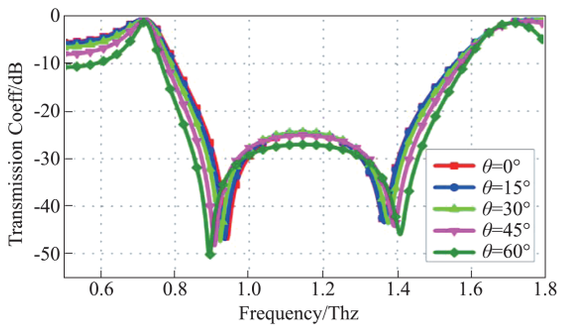

Fig. 5 The transmission spectrum for a wide-angle incidence from 0° to 60°
图5 入射角度从0°到60°度的透射谱

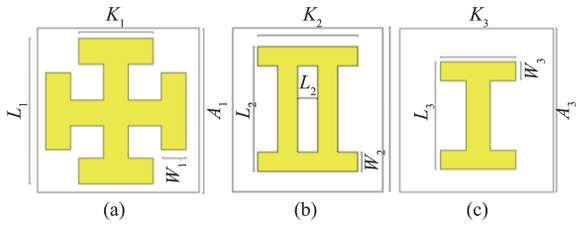

Fig. 6 Unit cell of several commonly used resonators (a) structure I, (b) structure II, and (c) structure III. Note: in Fig. 6, $A_1 = A_2 = A_3 = 80$ μm, $L_1 = 75$ μm, $L_2 = 60$ μm, $L_3 = 55$ μm, $K_1 = 40$ μm, $K_2 = 65$ μm, $K_3 = 50$ μm, $W_1 = W_2 = W_3 = 12$ μm
图6 几种常用谐振器的单元结构 (a)结构I,(b)结构II,(c)结构III. 图6中, $A_1 = A_2 = A_3 = 80$ μm, $L_1 = 75$μm, $L_2 = 60$ μm, $L_3 = 55$ μm, $K_1 = 40$ μm, $K_2 = 65$ μm, $K_3 = 50$ μm, $W_1 = W_2 = W_3 = 12$ μm

Table 1 Comparison of structures with compact arrays and traditional repetitive arrays
表1 基于紧凑阵列和传统周期阵列的对比

Performance	Structure Ⅰ		Structure Ⅱ		Structure Ⅲ	
	TF	CF	TF	CF	TF	CF
10 dB Bandwidth/GHz	220	282	520	790	410	480
Stopband Depth /dB	−33.0	−42.7	−54.8	−38.0	−40.6	−52.0
Slope of rising/ trailing edges (dB/THz)	252/ 175	467/ 320	313/ 183	318/ 328	247/ 107	418/ 156
resonant Point	1	2	2	2	1	2

CF represents double-layer filter structure based on compact array while TF stands for double-layer filter with traditional repetitive structure. Except for the structure II, other filters can excite an additional resonant point, causing a further improvement in bandwidth, slope of edges and stopband depth. More specifically, their bandwidth has been extended over 60 GHz, the stopband depth has been increased by about 10 dB, and the slope of the edge has increased by more than 50%. Although no extra resonant points are excited, compared with conventional design, the 10 dB bandwidth of structure II with compact design is widened by 270 GHz, and the sharpness of its edges can be also optimized. As shown in Table1, the TF filter based on structure II excites two resonant points. It is because structure II can be considered as a ring-like resonator and multilayer THz filter based on ring-like resonator can excite multiple resonances owing to its coupling behavior between layers. These numerical results indicate that the proposed filter with compact array can optimize filter performance by both exciting additional resonant mode and increasing the ability to receive EM waves. However, it is worth to mention that ring-like resonators or SRRs, exciting multiple resonant modes in multilayer design, cannot excite additional anti-symmetric mode by using compact arrays. It seems that compact arrays are only suitable for those structures that only excite a single dipole resonance in traditional repetitive design. The reason may be that these structures in multilayer design induce similar mode already. This also explains why no additional resonant mode is excited in structure II since its can be seen as a ring-like structure. Despite the limitations of compact array design, considering its mechanism to improve performance, it deserves to extend to the design of other THz device.

3 Conclusion

A THz filter based on compact array with the characteristics of broadband, polarization-independence, and angle insensitivity was proposed. The surface current density of designed filter is investigated to interpret the physics mechanism of the proposed with compact array. It is proven that a close arrays for cross-sharped metal layer in 2D level has more possibility to receive the THz waves, leading to a better performance in stopband depth. Moreover, in contrast to traditional design, owing to the asymmetry of the design structure, an additional resonant mode can be excited, causing a further improvement in bandwidth and the sharpness of cutting edges. The proposed cross-shaped filter with compact array has 750 GHz 10 dB bandwidth and sharp edges with slopes of 180 dB/THz and 258 dB/THz, respectively. Moreover, through parameter optimization, the transmission spectrum can keep nearly constant with a wider angle incidence range from 0° to 60°. In addition, the scheme of the filter with compact array can be expanded to the filter with different unit cells like Jerusalem cross, I-shaped, Ⅱ-shaped structures. With distinct advantage of angle independence, wider bandwidth, sharper edges and wide structure expansion, the proposed THz wave bandstop filter is suitable for the low-cost, complex application environment, integrated THz communication systems.

References

[1] Nagatsuma T, Ducournau G, Renaud C C. Advances in terahertz communications accelerated by photonics [J]. *Nature Photonics*, 2016, **10**: 371-379.
[2] Barros M T, Mullins R, Balasubramaniam S. Integrated terahertz communication with reflectors for 5G small-cell networks [J]. *IEEE Transactions on Vehicular Technology*, 2017, **66**(7): 5647-5657.
[3] Liu H B, Zhong H, Karpowicz N, *et al*. Terahertz spectroscopy and imaging for defense and security applications [J]. *Proceedings of the IEEE*, 2017, **95**(8): 1514-1527.

[4] Sun Y, Sy M Y, Wang Y J, *et al*. A promising diagnostic method: Terahertz pulsed imaging and spectroscopy [J]. *World Journal of Radiology*, 2011, **3**(3): 55-65.
[5] Yang X, Zhao X, Yang K, *et al*. Biomedical applications of terahertz spectroscopy and imaging [J]. *Trends in Biotechnology*, 2016, **34**(10): 810-824.
[6] Kim S M, Baughman W, Wilbert D S, *et al*. High sensitivity and high selectivity terahertz biomedical imaging [J]. *Chinese Optics Letters*, 2011, **9**(11): 110009.
[7] Oh S J, Kim S H, Jeong K Y, *et al*. Measurement depth enhancement in terahertz imaging of biological tissues [J]. *Optics Express*, 2013, **21**(18): 21299-21305.
[8] Dickie R, Cahill R, Fusco V, *et al*. THz frequency selective surface filters for earth observation remote sensing instruments [J]. *IEEE Transactions on Terahertz Science and Technology*, 2011, **1**(2): 450-461.
[9] Veselago V G. The electrodynamics of substances with simultaneously negative values of and μ [J]. *Soviet Physics Uspekhi* , 1968, **10**(4): 509-514.
[10] Pendry J B, Holden A J, Stewart W J, *et al*. Extremely low frequency plasmons in metallic mesostructures [J]. *Physical Review Letters*, 1996, **76**(25): 4773-4776.
[11] Hussein M, Zhou J, Huang Y, *et al*. Low-profile second-order terahertz bandpass frequency selective surface with sharp transitions: proceedings of 2017 10th UK-Europe-China Workshop on Millimetre Waves and Terahertz Technologies, 2017 [C]. UK, [s.n], 2017.
[12] Park D J, Park S J, Yoon S A N, *et al*. Dielectric constant measurements of thin films and liquids using terahertz metamaterials [J]. *RSC Advances*, 2016, **6**(73): 69381-69386.
[13] Qiu K, Jin J, Liu Z, *et al*. A novel thermo-tunable band-stop filter employing a conductive rubber split-ring resonator [J]. *Materials & Design*, 2017, **116**(15): 309-315.
[14] Ebrahimi A, Nirantar S, Withayachumnanku, *et al*. Al-sarawi and derek abbott. second-order terahertz bandpass frequency selective surface with miniaturized elements [J]. *IEEE Transactions on Terahertz Science and Technology*, 2015, **5**(5): 761-769.
[15] Kaya S. Windmill-shaped subwavelength apertures operating in the mid-IR regime [J]. *IEEE Transactions on Nanotechnology*, 2014, **13**(6): 1250-1256.
[16] Degiron A, Lezec H J, Barnes W L, *et al*. Effects of hole depth on enhanced light transmission through subwavelength hole arrays [J]. *Applied Physics Letters*, 2002, **81**(23): 4327-4329.
[17] J, Huang T, Liu P. Tunable polarization-independent terahertz band-stop filter based on graphene metasurface: proceedings of 2018 43rd International Conference on Infrared, Millimeter, and Terahertz Waves, 2018 [C]. Japen, [s.n], 2018.
[18] Chiang Y, Yang C, Yang Y, *et al*. An ultrabroad terahertz bandpass filter based on multiple-resonance excitation of a composite metamaterial [J]. *Applied Physics Letters*, 2011, **99**(19): 191909.
[19] Khodaee M, Banakermani M, Baghban H. GaN-based metamaterial terahertz bandpass filter design: tunability and ultra-broad passband attainment [J]. *Applied Optics*, 2015, **54**(29): 8617-8624.
[20] Al-Naib I, Born N, Koch M. Polarization and angle independent terahertz metamaterials with high Q-factors [J]. *Applied Physics Letters*, 2011, **98**(9): 091107.
[21] Ferraro A, Zografopoulos D C, Caputo R, *et al*. Angle-resolved and polarization-dependent investigation of cross-shaped frequency- selective surface terahertz filters [J]. *Applied Physics Letters*, 2017, **110**(14): 141107.
[22] Qi L, Li C. Multi-band terahertz filter with independence to polarization and insensitivity to incidence angles [J]. *Journal of Infrared, Millimeter, and Terahertz Waves*, 2015, **36**(11): 1137-1144.
[23] Franklin D, Chen Y, Vazquez-Guardado A, *et al*. Polarization-independent actively tunable colour generation on imprinted plasmonic surfaces [J]. *Nature Communications*, 2015, **6**:7337.
[24] Pendry J B, Martin-Moreno L, Garcia-Vidal F J. Mimicking surface plasmons with structured surfaces [J]. *Science*, 2004, **305**(5685): 847-848.
[25] Chase S T, Joseph R D. Resonant array bandpass filters for the far infrared [J]. *Applied Optics*, 1983, **22**(11): 1775-1779.
[26] Gao M, Mohamad S, Momeni A, *et al*. A hybrid miniaturized-element frequency selective surface with a third-order bandpass response [J]. *IEEE Antennas and Wireless Propagation Letters*, 2017, **16**: 708-711.
[27] Munk B A. *Frequency selective surfaces: Theory and design* [M]. USA: John Wiley & Sons, Inc, 2009.
[28] Paul O, Imhof C, Reinhard B, *et al*. Negative index bulk metamaterial at terahertz frequencies [J]. *Optics Express*, 2008, **16**(9): 6736-6744.
[29] Fedotov V A, Rose M, Prosvirnin S L, *et al*. Sharp trapped-mode resonances in planar metamaterials with a broken structural symmetry [J]. *Physical Review Letters*, 2007, **99**(14): 147401.
[30] Papasimakis N, Fedotov V A, Zheludev N I, *et al*. Metamaterial analog of electromagnetically induced transparency [J]. *Physical Review Letters*, 2008, **101**(25): 253903.
[31] Lukyanov A, Andrienko D. Extracting nondispersive charge carrier mobilities of organic semiconductors from simulation of small systems [J]. *Physical Review B*, 2010, **82**(19): 193202.
[32] Li X, Yang L, Hu C, *et al*. Tunable bandwidth of band-stop filter by metamaterial cell coupling in optical frequency [J]. *Optics Express*, 2011, **19**(6): 5283-5289.
[33] Lu M, Li W, Brown E R. Second-order bandpass terahertz filter achieved by multilayer complementary metamaterial structures [J]. *Optics Letters*, 2011, **36**(7): 1071-1073.
[34] Decker M, Zhao R, Soukoulis C M, *et al*. Twisted split-ring-resonator photonic metamaterial with huge optical activity [J]. *Optics Letters*, 2010, **35**(10): 1593-1595.